Supporting information for

Equilibrating (L)Fe^{III}–OOAc and (L)Fe^{V}(O) Species in Hydrocarbon Oxidations by Bio-Inspired Nonheme Iron Catalysts Using H_2O_2 and AcOH

Williamson N. Oloo,[a] Rahul Banerjee,[b] John D. Lipscomb,[b,*] and Lawrence Que, Jr.[a,*]

[a]Department of Chemistry and Center for Metals in Biocatalysis, University of Minnesota, Minneapolis, MN 55455 (United States). E-mail: larryque@umn.edu

[b]Department of Biochemistry, Molecular Biology, and Biophysics and Center for Metals in Biocatalysis, University of Minnesota, Minneapolis, MN 55455 (United States). E-mail: lipsc001@umn.edu

(a)

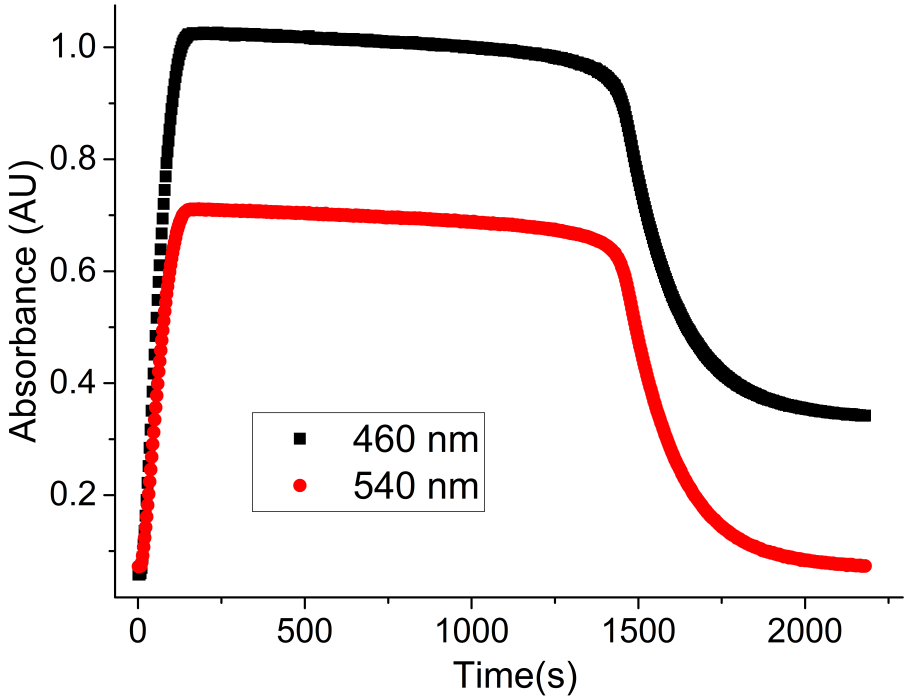
1.0
0.8
0.6
0.4
0.2
Absorbance (AU)
460 nm
540 nm
0
500
1000
1500
2000
Time(s)

(b)

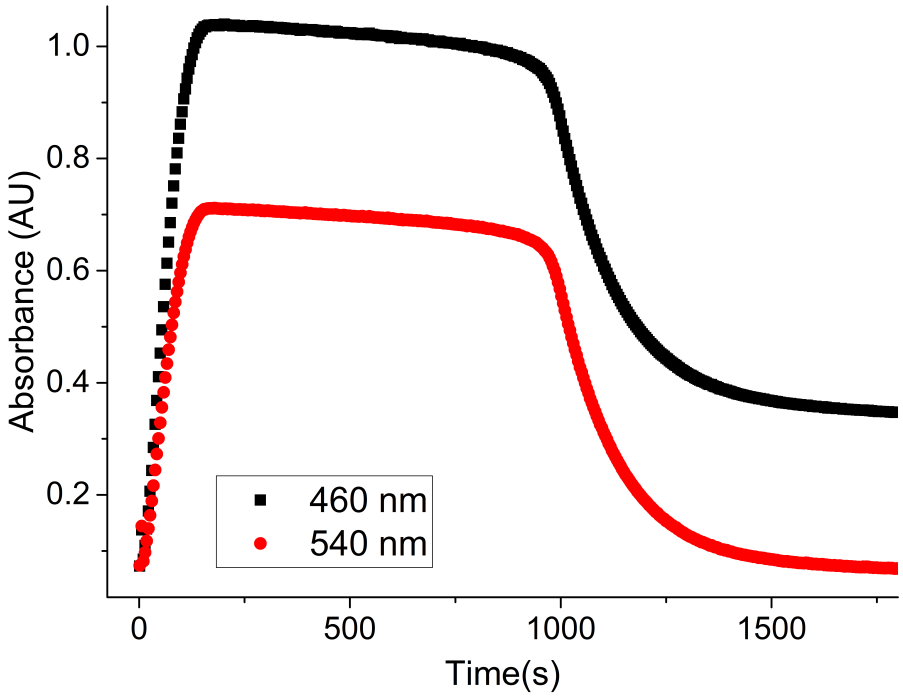
1.0
0.8
0.6
0.4
0.2
Absorbance (AU)
460 nm
540 nm
0
500
1000
1500
Time(s)

(c)

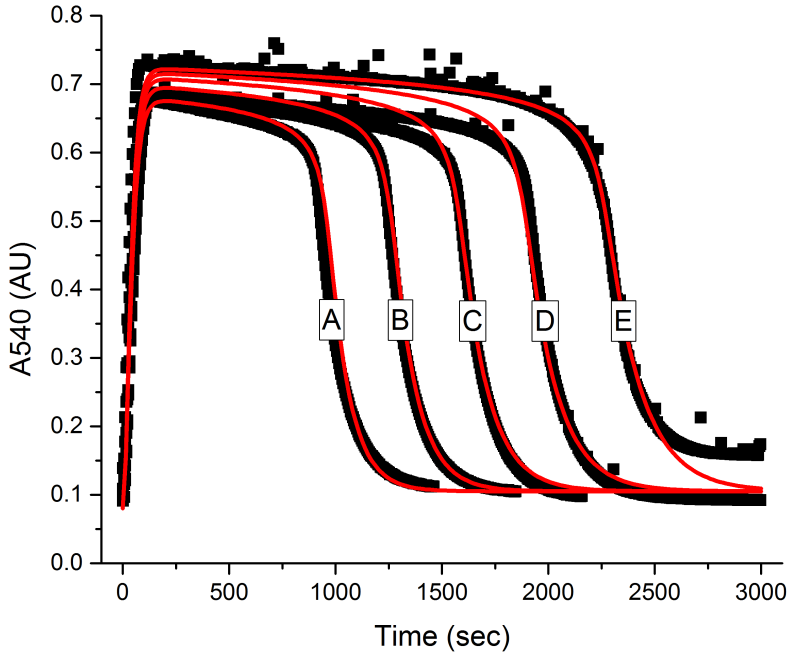

Figure S1. Kinetic time traces of a catalytic oxidation reaction involving **1a*** (0.5 mM), H_2O_2 (10 mM), and AcOH (100 mM) in CH_3CN at -40 °C showing the formation and decay of **3a*** as monitored at 460 nm (black trace) and 540 nm (red trace) in the presence of 100 equivalents (a) and 400 equivalents (b) of 1-octene. The two time traces shown in each panel evolve identically as a function of time, demonstrating that the kinetic evolution of this species does not depend on which of the two wavelengths are monitored but is sensitive to the amount of substrate present. (c) Numerical simulation fitting (red traces) of the kinetic traces for **3a*** at 540 nm. The numbers of equivalents of 1-octene used were 400 (A), 200 (B), 100 (C), 50 (D) and 0 (E) relative to **1a*** catalyst. The model (Scheme 2) with the rate constants (Table 4) derived from fitting the kinetic data at 460 nm were successfully able to reproduce this kinetic data.

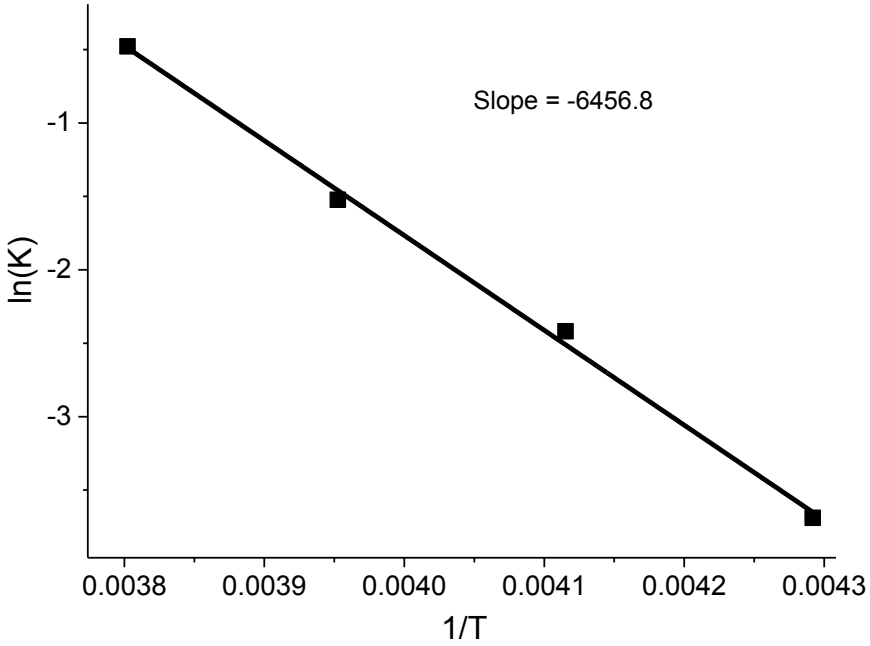

Figure S2a. Arrhenius plot for epoxide formation in the reaction involving 1 mM of **1a***, 200 equiv. AcOH, 20 equiv. HOOH, and 200 equiv. of 1-octene. This plot affords an activation energy of 54(2) kJ/mol.

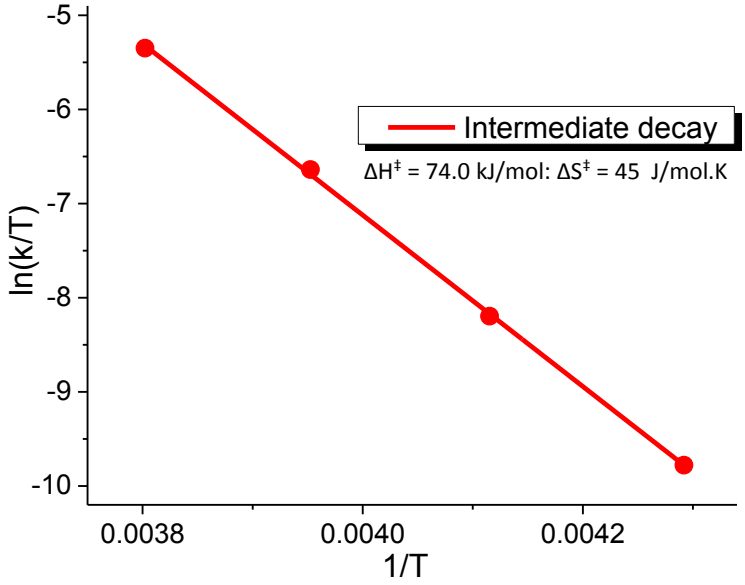

Figure S2b. Eyring plot for the decay of **2a*** in the reaction involving 1 mM of **1a***, 200 equiv. AcOH, 20 equiv. HOOH, and 200 equiv. of 1-octene. This plot affords an activation enthalpy of 74.0 kJ/mol and an activation entropy of 45 J/mol.K.

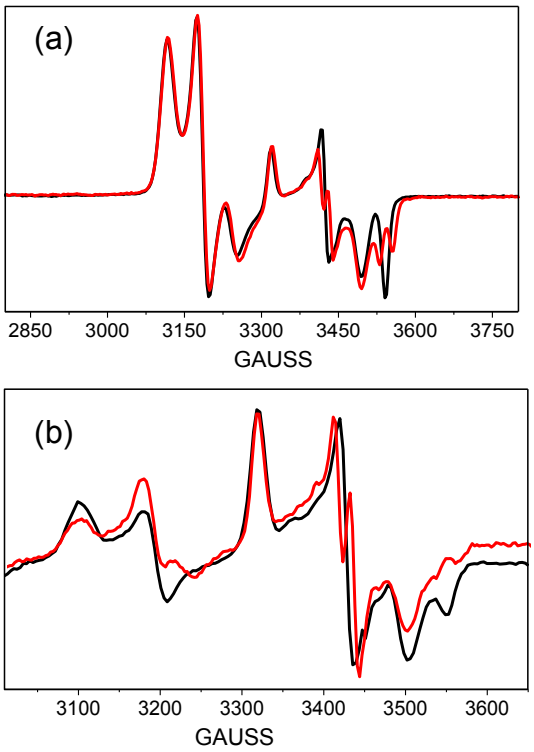

Figure S3. EPR spectra of the reaction mixture of 1 mM **1a** (a) and 1 mM **1a*** (b) with 5 equiv. AcOOH in acetonitrile/acetone mixtures at -50 °C frozen at the maximum accumulation of either **3a** or **3a***, as monitored by the 460 nm UV-vis chromophore. Black spectra represent ^{56}Fe solutions while red spectra show ^{57}Fe solutions. EPR conditions: T = 20 K, 0.2 mW, 1 mT modulation amplitude.

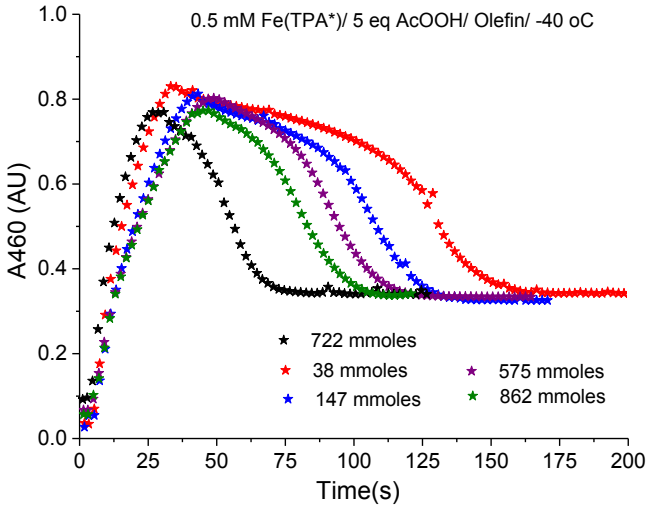

Figure S4. Kinetic time trace for the evolution of **3a*** (monitored at 460 nm) generated using 0.5 mM of **1a*** and 5 equiv. AcOOH at -40 °C in the presence of various equivalents of 1-octene. It is clear that the presence of 1-octene decreases the lifetime of **3a*** significantly.

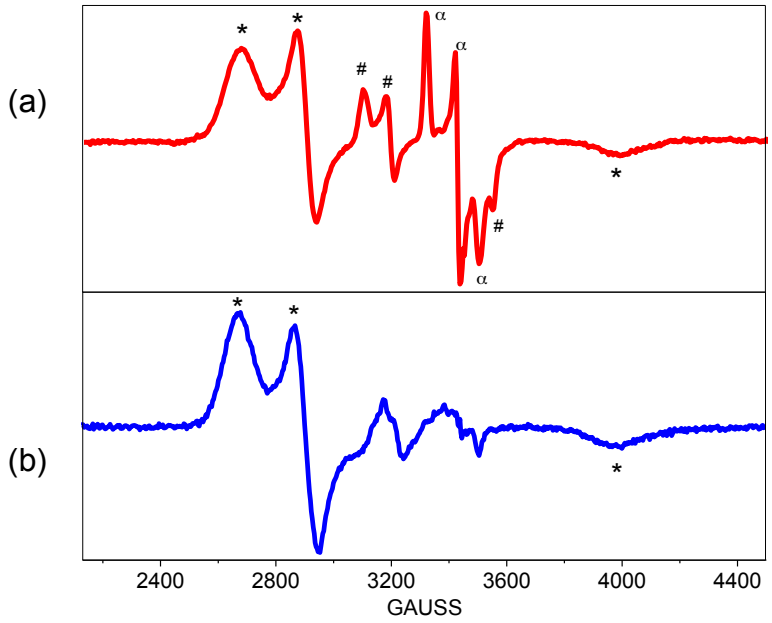

Figure S5. (a) EPR spectrum of a frozen mixture of **1a*** and AcOOH (20 equiv.) in CH_3CN at -40 °C upon maximum accumulation of the 460 nm chromophore, showing **3a*** at g = 2.58, 2.38, 1.73 (*), **5a*** at g = 2.07, 2.01, 1.96 (α), and **6a*** at g = 2.21, 2.16, 1.94 (#). (b) EPR spectrum of a mixture of **1a*** and AcOOH in the presence of 1-octene (50 equiv.) showing signals of **3a*** (*). It is clear that the presence of 1-octene causes the signals belonging to **5a*** (α) and **6a*** (#) to disappear. EPR conditions: T = 20K, 0.2 mW, 1 mT modulation amplitude.

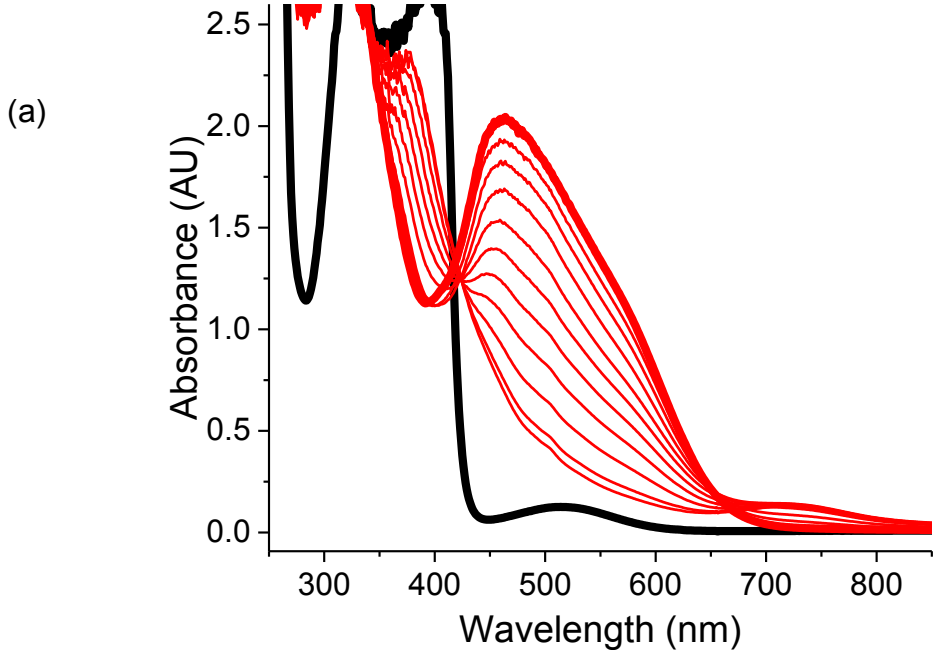

(b)

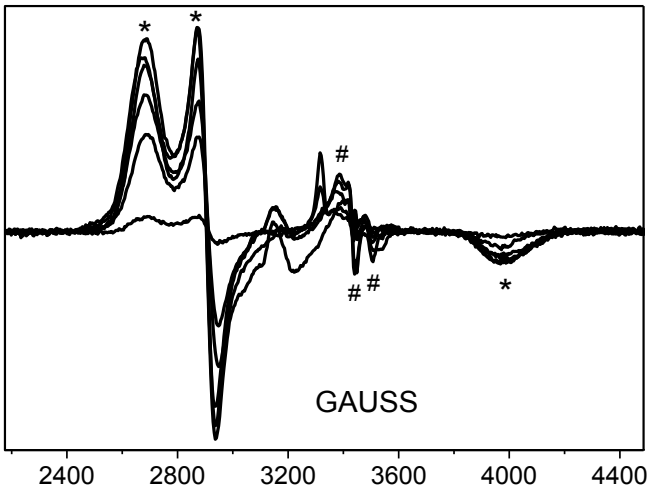

Figure S6. Combination of a 1 mM solution of **1a***, 20 equiv. H_2O_2 and 200 equiv. AcOH in CH_3CN at -40 °C. (a) UV-visible spectra for the reaction mixture showing accumulation and decay of **3a***. (b) EPR spectra of the reaction mixture as a function of time. From this figure, signals belonging to **2a*** (indicated by #) and **3a*** (indicated by *) accumulate and then decay completely during the time period examined.

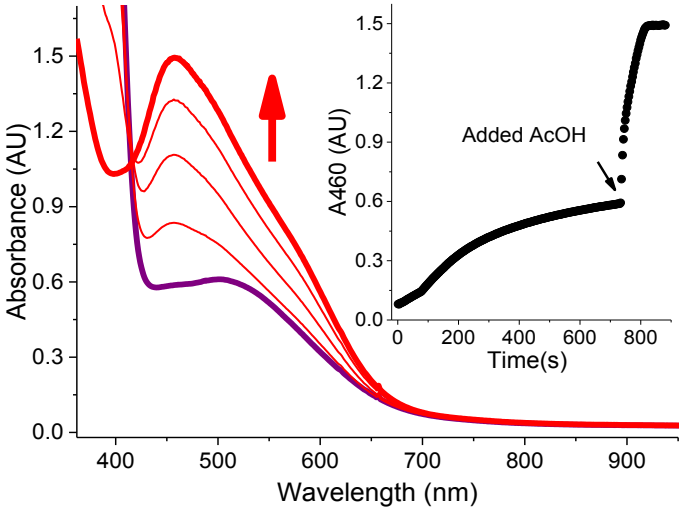

Figure S7. Spectral changes upon addition of 200 equiv. AcOH to a 0.8 mM CH_3CN solution of **2a*** (purple trace) at -40 °C. As the absorption bands of **2a*** and **3a*** overlap to a large degree, the UV-vis spectral changes upon **2a*** decay to form **3a*** involves primarily an increase in absorbance and a shift in λ_{max} to 460 nm. Inset: Time-trace for the formation of **3a*** monitored at 460 nm. The non-exponential formation of **3a*** upon addition of an excess amount of AcOH to a solution of **2a*** is indicative of a transformation that is not straightforward. The extensive overlap between the chromophores of **2a*** and **3a*** masks the observation of an intermediate during this transformation. The presence of such an intermediate is more obvious in reactions that involve **2a** and AcOH, because the chromophores of **2a** and **3a** do not overlap to a significant extent.

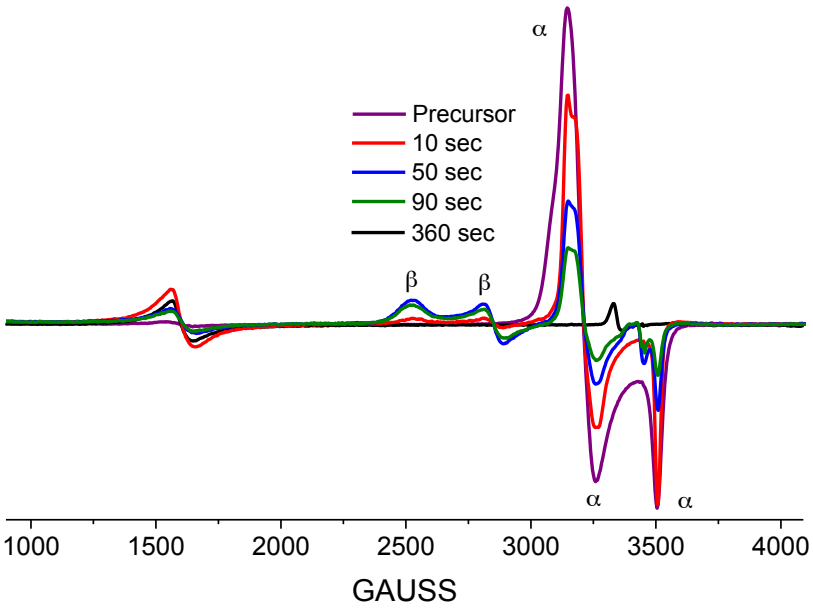

Figure S8. The addition of 200 equiv. of AcOH to the (TPA)Fe^{III}–OOH complex **2a** (α), which was generated by adding HOOH (20 equiv.) to a 1-mM solution of **1a** in CH_3CN at -40 °C, afforded the (TPA)Fe^{III}(OOAc) complex **3a** (β), which eventually decays. EPR analysis of aliquots of this reaction mixture collected at various timepoints (indicated in the figure). EPR conditions: T = 20K, 0.2 mW, 1 mT modulation amplitude.

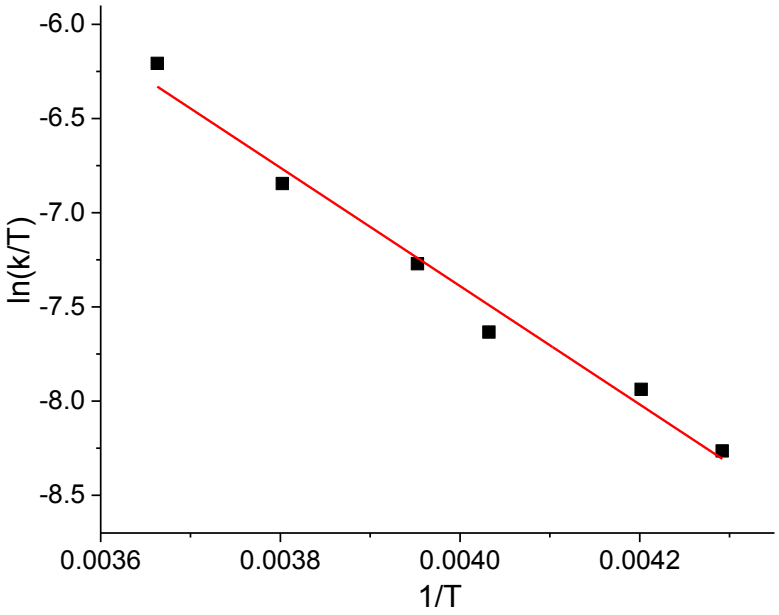

Figure S9. Eyring plot for the decay of **2a** in the presence of 200 equiv. AcOH. This plot affords an activation enthalpy of 25(2) kJ/mol and activation entropy of -151(10) J/mol•K.

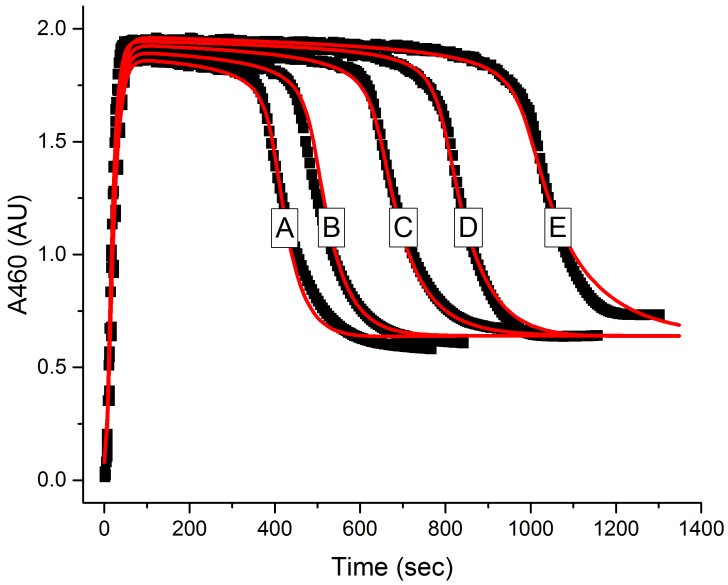

Figure S10. Numerical simulation fits (red traces) to the experimental kinetic time courses (black traces) of **3a*** (460 nm) generated by adding 10 mM H_2O_2 and 200 mM AcOH to 1 mM **1a*** in CH_3CN at -40 °C. The different kinetic traces represent reactions in the presence of various substrate types and concentrations. A = 250 mM 1-octene; B = 125 mM 1-octene; C = 62.5 mM 1-octene; D = 250 mM cyclohexane; E = no substrate.

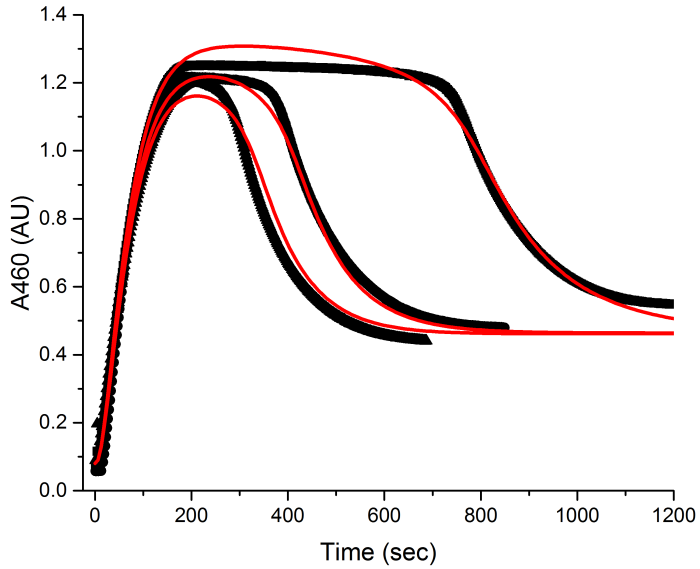

Figure S11. Numerical simulation fits (red traces) to the experimental kinetic time courses (black traces) of **3a*** (460 nm) generated by adding 10 mM H_2O_2 and 100 mM AcOH to 0.65 mM **1a*** in CH_3CN at -40 °C. The different kinetic traces represent reactions in the presence of various concentrations of cyclohexadiene. The traces from right to left correspond to 10, 25 and

50 equiv. of cyclohexadiene added. All fitted rate constants in Scheme 2 remain identical to the values obtained from fitting the reaction in the presence of 1-octene (Table 4), except the rate constant of substrate oxidation (k_8 = 88 M^{-1} s^{-1}).

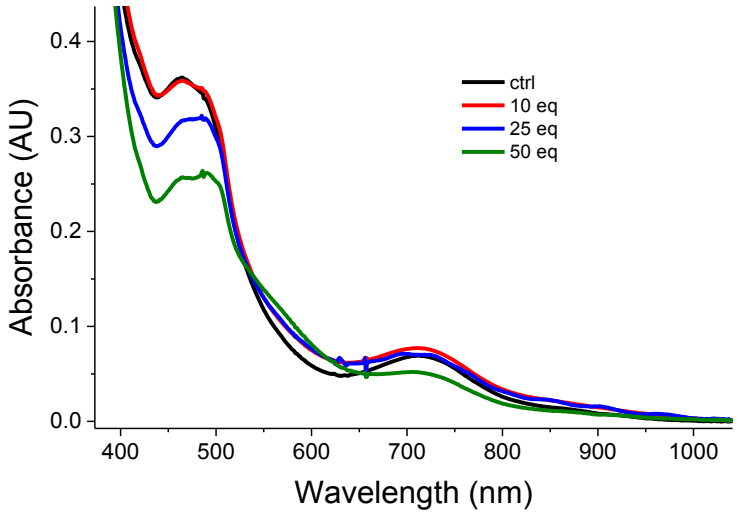

Figure S12. The UV-vis traces of **3a** at steady state generated by adding 20 equiv. HOOH to a 0.5 mM solution of **1a** in CH_3CN at -40 °C in the presence of 200 equiv. AcOH and 0 – 50 equiv. of 1-octene, showing the variation in the yield of **3a** as a function of 1-octene concentration.

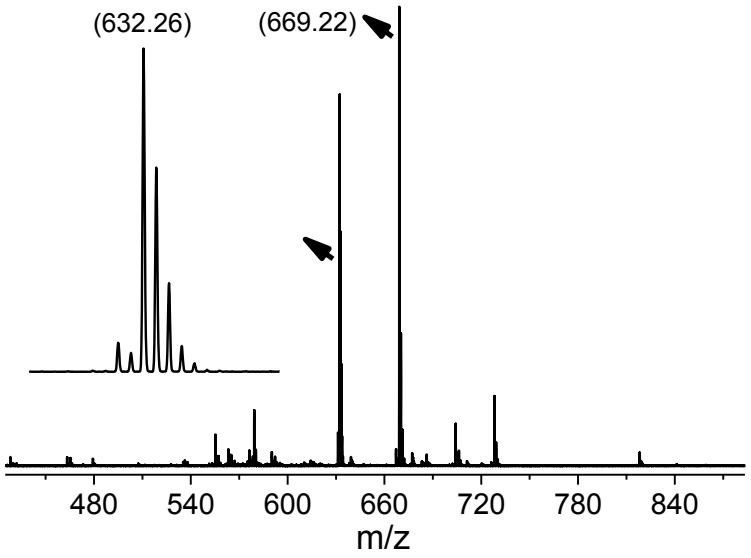

Figure S13. ESI-MS spectrum of the reaction mixture containing **1a** (0.5 mM), HOOH (20 equiv.), and AcOH (200 equiv.) upon decay of **3a** at -40 °C . The m/z at 632.26 corresponds to the dicationic, diferric species supported by TPA* with oxo- and acetato-bridges, along with a triflate counterion. The peak at m/z = 669.22 corresponds to the monocationic $(L)Fe^{II}$ precursor.

Global fitting of the data shown in Figure 11.

The experimental data in Figure 11 were globally fit to the chemical models described in Scheme S1 (same as Scheme 2 in main text) through a numerical simulation method in the program KinTek Explorer. The primary species with absorption at 460 nm is Fe^{III}–OOAc (**3a***) while the diiron species 7 (Scheme S1) also absorbs at this wavelength ($1/6^{th}$ of the extinction coefficient of **3a***). Initial estimates for rate constants are obtained via the dynamic simulation method in the program where individual rate constants in the model are altered until a reasonable fit is obtained to the experimental kinetic curves. The program then performs a nonlinear regression to find the optimal fit for all parameters by fitting directly to the model based upon a numerical integration of the rate equations and the starting condition for each experiment. The program seeks the minimum chi^2 value iteratively. The fitting scheme also recognizes that the rate constants of some chemical steps may not be constrained by the experimental data and thus provides lower and upper bounds for each rate constant computed from a 1.2 x chi-square multiple of the final fit.

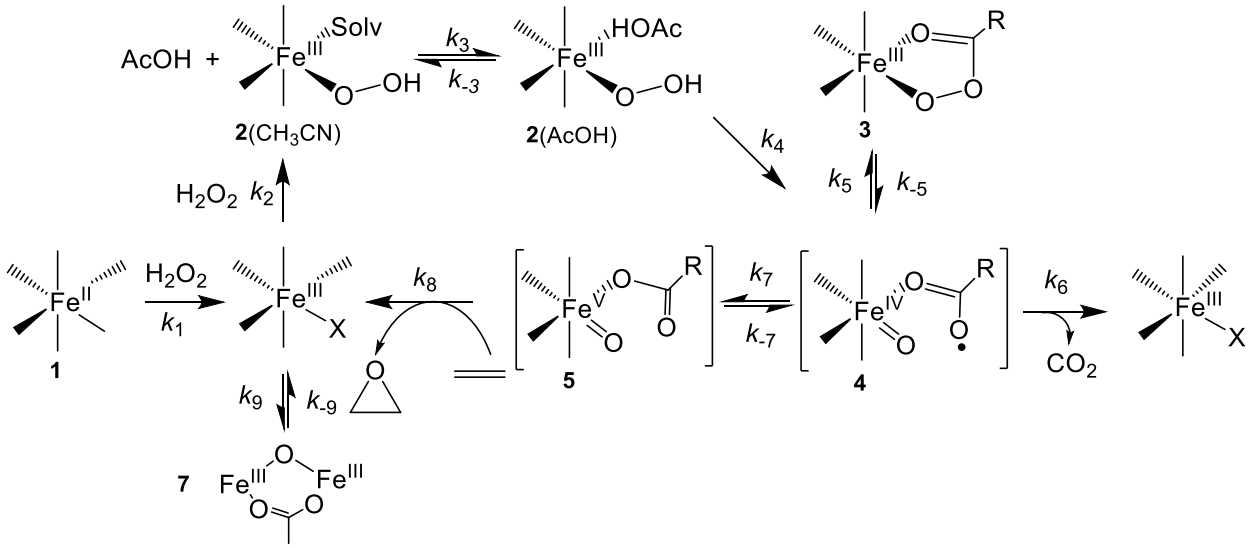

Scheme S1. Chemical model used to fit the kinetic evolution of **3a*** (460 nm) as a function of 1-octene concentration shown in **Figure 11**.

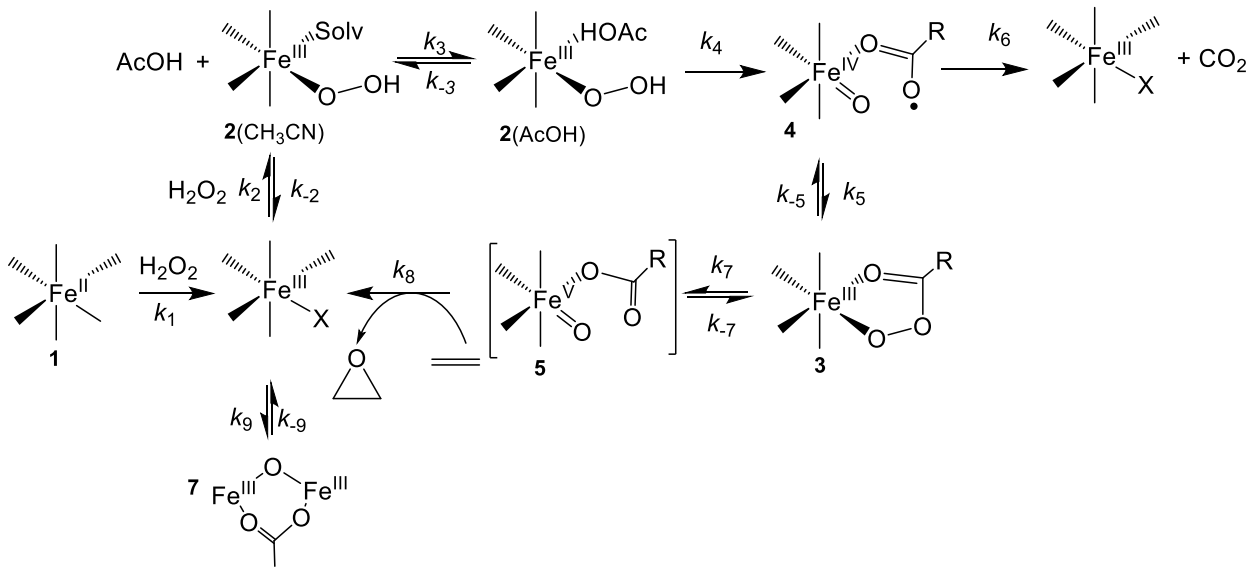

Scheme S2. Alternative chemical model used to fit the kinetic evolution of **3a*** (460 nm) as a function of 1-octene concentration shown in Figure 11. This model includes a heterolytic cleavage of **3a*** to generate **5a***. This simulation does not reproduce the experimental data of Figure 11.

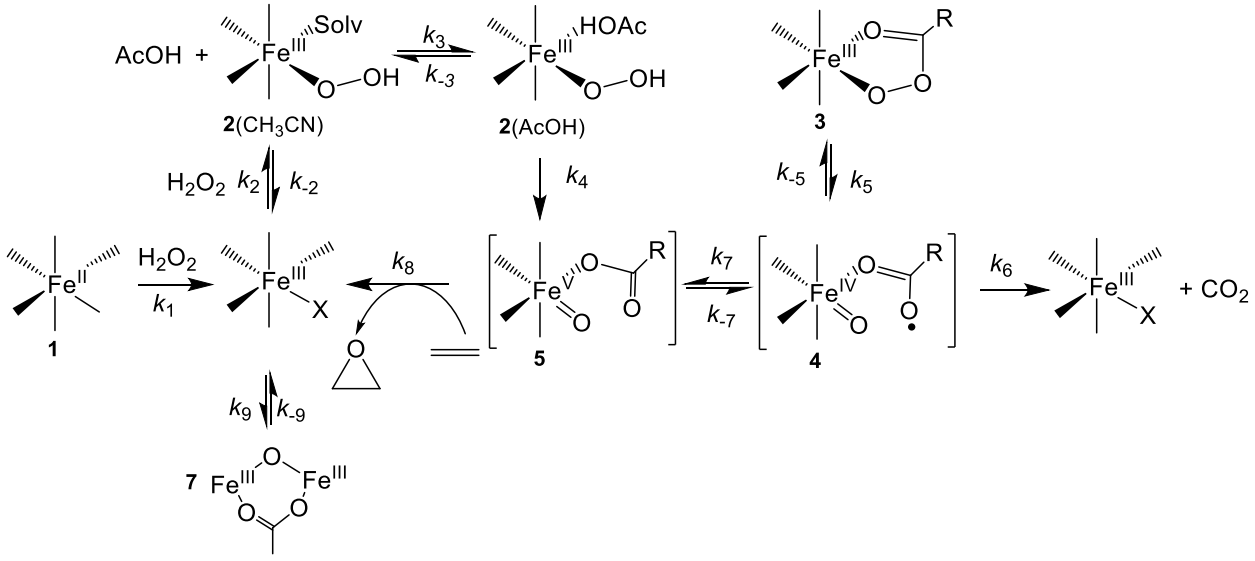

Scheme S3. An alternative chemical model used to fit the kinetic evolution of **3a*** (460 nm) as a function of 1-octene concentration shown in Figure 11. This model also includes an acid-assisted heterolytic cleavage of **2a*** to afford **5a***, which then exists in a reversible equilibrium with **4a*** and **3a***. This model however does not reproduce the data in Figure 11.